

# C<sub>60</sub>O<sub>3</sub>, a Fullerene Ozonide: Synthesis and Dissociation to C<sub>60</sub>O and O<sub>2</sub>

Dieter Heymann,<sup>\*,†</sup> Sergei M. Bachilo,<sup>‡</sup> R. Bruce Weisman,<sup>‡</sup> Franco Cataldo,<sup>#</sup>  
Roelof H. Fokkens,<sup>§</sup> Nico M. M. Nibbering,<sup>§</sup> Ronald D. Vis,<sup>⊥</sup> and L. P. Felipe Chibante<sup>†</sup>

Contribution from the Department of Geology and Geophysics, Rice University, Houston, Texas 77251-1892, Department of Chemistry and Rice Quantum Institute, Rice University, Houston, Texas 77251-1892, Soc. Lupi Chemical Research Institute, Via Casilina 1626/A, 00133 Rome, Italy, Institute of Mass Spectrometry, University of Amsterdam, 1018 WS Amsterdam, The Netherlands, and Department of Physics and Astronomy, Free University, 1081 HV Amsterdam, The Netherlands

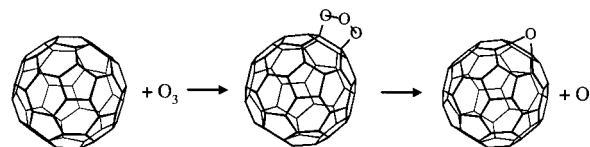
Received July 13, 2000

**Abstract:** An unstable intermediate has been detected and isolated in the reaction of ozone with C<sub>60</sub> in solution. On the basis of its UV–vis absorption spectrum, the measured release of O<sub>2</sub> in its decay to the epoxide C<sub>60</sub>O, and the first-order kinetics of this reaction, the intermediate has been identified as C<sub>60</sub>O<sub>3</sub>, a primary ozonide. This [6,6]-closed adduct of ozone with C<sub>60</sub> thermally dissociates to C<sub>60</sub>O plus O<sub>2</sub> in toluene solution, octane solution, and the solid phase with rate constants (at 23 °C) of  $4.6 \times 10^{-2}$ ,  $1.3 \times 10^{-3}$ , and  $3.0 \times 10^{-3} \text{ min}^{-1}$ , respectively. The activation energy for dissociation in toluene solution is approximately 89 kJ mol<sup>-1</sup>. Semiempirical quantum calculations indicate that the formation and subsequent dissociation of C<sub>60</sub>O<sub>3</sub> are both exothermic processes. These findings constitute the first observation of a fullerene ozonide.

## Introduction

Compounds of C<sub>60</sub> with oxygen have been of prime interest since the early days of fullerene chemistry.<sup>1</sup> The first derivative of C<sub>60</sub>, reported in 1992, was the epoxide [6,6]-closed C<sub>60</sub>O.<sup>1a</sup> In 1993, Chibante and Heymann discovered the swift and complex reaction of ozone with C<sub>60</sub> in toluene solution to form products that include C<sub>60</sub>O, higher oxides of composition C<sub>60</sub>O<sub>2</sub> through C<sub>60</sub>O<sub>6</sub>, and insoluble tan-colored precipitates.<sup>1b</sup> Despite this rich chemistry, the mechanisms of oxide formation in fullerenes have remained unresolved. We report here the

discovery of a hitherto unrecognized intermediate (denoted here as C<sub>60</sub>X) formed by the ozonation of C<sub>60</sub> in hydrocarbon solutions. This intermediate is observed to produce C<sub>60</sub>O in toluene and octane solutions, and in the solid state. Kinetic, spectroscopic, and photophysical studies of C<sub>60</sub>X have allowed us to identify this intermediate species as C<sub>60</sub>O<sub>3</sub>, a [6,6]-closed primary ozonide of C<sub>60</sub>, and to find the activation energy for its dissociation into C<sub>60</sub>O plus molecular oxygen. The deduced ozonide formation and decay steps are illustrated below as reaction 1.



Our findings clarify the mechanism of the most efficient process for oxygenation of fullerenes and suggest a formation route for the polymeric products of ozonation.

## Experimental Section

**Materials.** C<sub>60</sub> was obtained from Bucky USA. HPLC analysis indicated no detectable C<sub>70</sub> contamination and less than 0.5% C<sub>60</sub>O content. Ozone was generated in a carrier stream of O<sub>2</sub> by electrical discharge. All solvents used were HPLC grade or redistilled. Solutions were filtered through 0.2 μm PTFE filters to remove precipitates.

**HPLC Analyses.** Analyses of all solutions for C<sub>60</sub>, C<sub>60</sub>X, and known fullerene oxides were performed by HPLC with a Nacal Tesque "Cosmosil Buckyprep" 250 × 4.6 mm column that was cooled with ice to retard the decay of C<sub>60</sub>X during analysis.<sup>2</sup> With this column, the C<sub>60</sub> diepoxide isomer known as C<sub>60</sub>O<sub>2</sub>[I] shows a longer retention time than the C<sub>60</sub>O<sub>2</sub>[II] isomer.<sup>1g,h,j</sup> Toluene was used as the mobile phase

(2) Approximately 7% of the C<sub>60</sub>X decayed during the analysis.

\* To whom correspondence should be addressed.

<sup>†</sup> Rice University, Department of Geology and Geophysics.

<sup>‡</sup> Rice University, Department of Chemistry.

<sup>#</sup> Soc. Lupi Chemical Research Institute.

<sup>§</sup> University of Amsterdam.

<sup>⊥</sup> Free University.

(1) (a) Creagan, K. M.; Robbins, J. L.; Robbins, W. K.; Millar, J. M.; Sherwood, R. D.; Tindall, P. J.; Cox, D. M.; Smith, A. B., III; McCauley, J. P., Jr.; Jones, D. R.; Gallagher, R. T. *J. Am. Chem. Soc.* **1992**, *114*, 1103–1105. (b) Chibante, L. P. F.; Heymann, D. *Geochim. Cosmochim. Acta* **1993**, *57*, 1879–1881. (c) McElvany, S. W.; Callahan, J. H.; Ross, M. M.; Lamb, L. D.; Huffman, D. R. *Science* **1993**, *260*, 1632–1634. (d) Chibante, L. P. F. Ph.D. Thesis Rice University, 1994, pp 52–59. (e) Balch, A. L.; Costa, D. A.; Noll, B. C.; Olmstead, M. M. *J. Am. Chem. Soc.* **1995**, *117*, 8926–8932. (f) Cataldo, F.; Ori, O. *Polym. Degradation Stability* **1995**, *48*, 291–296. (g) Deng, J.-P.; Mou, C.-Y.; Han C.-C. *Proc. Electrochem. Soc.* **1995**, *95–10*, 1409–1424. (h) Deng, J.-P.; Mou, C.-Y.; Han C.-C. *J. Phys. Chem.* **1995**, *99*, 14907–14910. (i) Hamano, T.; Mashino, T.; Hirobe, M. *J. Chem. Soc., Chem. Commun.* **1995**, 1537–1538. (j) Deng, J.-P.; Mou, C.-Y.; Han C.-C. *Proc. Electrochem. Soc.* **1996**, *96–10*, 146–153. (k) Lebedkin, S.; Ballenweg, S.; Gross, J.; Taylor, R.; Kraetschmer, W. *Tetrahedron Lett.* **1995**, *36*, 4971–4974. (l) Davydov, V. Ya.; Filatova, G. N.; Knipovich, O. M.; Lunin, V. V. *Proc. Electrochem. Soc.* **1996**, *96–10*, 1295–1307. (m) VanCleave, A.; Gijbels, R.; Van den Heuvel, H.; Claeys M. *Proc. Electrochem. Soc.* **1997**, *97–14*, 783–800. (n) Krause, M.; Dunsch, L.; Seifert, G.; Fowler, P. W.; Gromov, A.; Kraetschmer, W.; Gutierrez, R.; Porezag, D.; Fraunheim, T. *J. Chem. Soc., Faraday Trans.* **1998**, *94*, 2287–2294. (o) Barrow, M. P.; Tower, N. J.; Taylor, R.; Drewello, T. *Chem. Phys. Lett.* **1998**, *293*, 302–308. (p) Shang, Z.; Pan, Y.; Cai, Z.; Zhao, X.; Tang, A. *J. Phys. Chem. A* **2000**, *104*, 1915–1919.

**Table 1.** Summary of HPLC Kinetic Experiments

run	solvent	temp (°C)	initial species	final species	<i>k</i> (min <sup>-1</sup> )	<i>k'</i> (min <sup>-1</sup> )
1	toluene	23.0	C <sub>60</sub> X <sup>a</sup>	C <sub>60</sub> O	0.0455	0.0461
2	toluene	23.0	C <sub>60</sub> X <sup>a</sup>	C <sub>60</sub> O	0.0465	0.0455
3	toluene	14.2	C <sub>60</sub> X <sup>a</sup>	C <sub>60</sub> O	0.0208	0.0177
4	toluene	14.2	C <sub>60</sub> X <sup>a</sup>	C <sub>60</sub> O	0.0208	0.0178
5	toluene	9.9	C <sub>60</sub> X <sup>a</sup>	C <sub>60</sub> O	0.0096 <sup>d</sup>	
6	toluene	9.9	C <sub>60</sub> X <sup>a</sup>	C <sub>60</sub> O	0.00975	0.0133
7	toluene	0.4	C <sub>60</sub> X <sup>a</sup>	C <sub>60</sub> O	0.0022 <sup>d</sup>	
8	toluene	0.4	C <sub>60</sub> X <sup>a</sup>	C <sub>60</sub> O	0.00240	0.00238
9	toluene	23.0	C <sub>60</sub> X, C <sub>60</sub> <sup>a,b</sup>	C <sub>60</sub> O, <sup>c</sup> C <sub>60</sub> , C <sub>60</sub> O <sub>2</sub>	0.038 <sup>d</sup>	
10	toluene	23.0	C <sub>60</sub> X, C <sub>60</sub> <sup>a,b</sup>	C <sub>60</sub> O, <sup>c</sup> C <sub>60</sub> , C <sub>60</sub> O <sub>2</sub>	0.0424	
11	octane	23.0	C <sub>60</sub> X, C <sub>60</sub> <sup>a,b</sup>	C <sub>60</sub> O, <sup>c</sup> C <sub>60</sub> , C <sub>60</sub> O <sub>2</sub>	0.00126	
12	octane	40.1	C <sub>60</sub> X, C <sub>60</sub> <sup>a,b</sup>	C <sub>60</sub> O, <sup>c</sup> C <sub>60</sub> , C <sub>60</sub> O <sub>2</sub>	0.00642	

<sup>a</sup> Small quantities of C<sub>60</sub>O were present. <sup>b</sup> Small quantities of C<sub>60</sub>O<sub>2</sub>[II] were present. <sup>c</sup> Most abundant species. <sup>d</sup> Less reliable values.

with flow rates in the range of 1.5 to 2.0 mL/min.<sup>3</sup> A Waters model 996 photodiode array (PDA) provided UV–vis absorption detection from 300 to 600 nm. For quantitative work, peak areas and heights were determined in chromatograms constructed from absorbance measured at 330 nm. We compensated for small variations in instrument performance by normalizing the areas or heights of C<sub>60</sub>X peaks to the area or height of the C<sub>60</sub> peak when it was present in the chromatograms. When only C<sub>60</sub>X and C<sub>60</sub>O were present, signals were normalized instead to the sums of the areas or heights of these two peaks, which turned out to be nearly constant. To obtain better absorption spectra of eluted species between 300 and 750 nm, we used a Shimadzu HPLC instrument equipped with a Cosmosil 5PYE column and a model SPD-M10Avp photodiode array detector.

**HPLC Kinetic Studies.** Stock solutions of C<sub>60</sub> for ozonations were prepared in toluene (2 mg/mL), octane (20 μg/mL), and hexane (35 μg/mL).<sup>4</sup> These samples were mildly ozonized by bubbling a mixture of oxygen and ozone through them at 0 °C. After a purge with dry argon, the ozonized solutions were either used immediately or stored at –15 °C for later studies. Table 1 summarizes the conditions used for 12 kinetic experiments, in which the sample was held at the listed temperature while aliquots were regularly removed for HPLC analysis until essentially all of the C<sub>60</sub>X was transformed. Experiments 1 through 8 were carried out on purified fractions of C<sub>60</sub>X, whereas experiments 9 through 12 were performed on ozonized but unseparated solutions of C<sub>60</sub> in toluene and octane. Purifications were carried out by collecting the HPLC effluent from the PDA between the beginning and end of the C<sub>60</sub>X peak.

An additional set of experiments was performed to measure decay of C<sub>60</sub>X in the solid phase. Five separate 2 mL samples of the stock solution of C<sub>60</sub> in hexane were lightly ozonized at 0 °C. A 0.1 mL portion of each was immediately analyzed by HPLC. The solutions were then evaporated to dryness in less than 2 min and the residues were stored separately at 23 °C. Just before the selected sampling time, 1.5 mL of toluene was added to a sample to quickly dissolve all fullerenes, and a 0.1 mL portion of the resulting solution was immediately analyzed by HPLC. This analysis process was repeated at specific intervals with the remaining samples. C<sub>60</sub>, which was neither formed nor consumed in the reaction of C<sub>60</sub>X, was used as an internal standard to normalize the peak areas of C<sub>60</sub>O and C<sub>60</sub>X in these chromatograms.

**Mass Spectrometry of C<sub>60</sub>X.** Mass spectrometry promised the most direct method for determining the X in C<sub>60</sub>X. Because combined HPLC-MS instrumentation was not available, these two analytical methods were carried out side-by-side. One-microliter portions of ozonized C<sub>60</sub> solutions in toluene, hexane, or octane were evaporated on the gold-plated sample holder of a laser-desorption, time-of-flight mass spectrometer (Perseptive Biosystems; Voyager DE RP). The amounts of C<sub>60</sub> and C<sub>60</sub>X loaded on the sample holder were on the order of 10<sup>-6</sup> and 10<sup>-7</sup> g in the case of toluene, and on the order of 10<sup>-8</sup> and 10<sup>-9</sup> g in the case of the alkanes. The sample holder was then exposed to 3

ns, 6 to 8 μJ pulses from a 337 nm nitrogen laser. Time-of-flight mass spectra were measured in reflectron and linear modes. Comparison of spectra taken on different spots of the same deposit suggested that some fractionation had taken place during evaporation, because the signal ratios for masses 736/720 (C<sub>60</sub>O<sup>+</sup>/C<sub>60</sub><sup>+</sup>) varied somewhat. Simultaneously with the mass spectrometry, 0.1 mL of the same solution was injected into the HPLC system to determine the concentrations of compounds of interest.

**UV–vis Spectra of C<sub>60</sub>X.** A concentrated solution of purified C<sub>60</sub>X in toluene was prepared by HPLC separation. This sample was held briefly at –15 °C before being transferred to a fused silica cuvette in which it was allowed to warm to room temperature. Spectra were then taken in a Cary 4 double-beam spectrophotometer at 5 min intervals to monitor the transformation of C<sub>60</sub>X to products. The spectral slit width was set to 1.0 nm. After the measurement was completed, the composition of the solution was checked by HPLC analysis. UV–vis absorption spectra were also measured for separated HPLC fractions as they entered the photodiode array detector of the Shimadzu HPLC apparatus.

**Oxygen Determination.** To monitor the presence of molecular oxygen, we used the method of sensitized oxygen luminescence. Sample solutions were excited by 532 nm light pulses from a Q-switched Nd:YAG laser. This led to the prompt production of triplet state fullerenes that, if quenched by dissolved oxygen, generated the <sup>1</sup>Δ<sub>g</sub> excited state of O<sub>2</sub>. Characteristic 1270 nm luminescence from such excited oxygen molecules was detected by an amplified Ge photodiode following a grating monochromator. The output of the detector was recorded by a Tektronix TDS-430A digitizing oscilloscope and averaged over several hundred excitation shots to improve the signal-to-noise ratio. This detection system had a time resolution of approximately 1.5 μs.

In our oxygen determination runs, a saturated solution of C<sub>60</sub> in toluene was carefully ozonized to obtain a C<sub>60</sub>X concentration near 300 μM.<sup>5</sup> A 0.5 mL portion of this solution was quickly purified by HPLC to obtain a 2 mL fraction of pure C<sub>60</sub>X, which was then mixed with 2 mL of a saturated toluene solution of C<sub>60</sub>. This C<sub>60</sub> was added as a sensitizer of oxygen luminescence. Before the start of the run, the sample was kept at –15 °C whenever possible so as to prevent premature transformation of C<sub>60</sub>X. Initially dissolved atmospheric oxygen was removed from the sample solution by four cycles of freeze–pump–thaw degassing. The sealed, degassed sample was then warmed to room temperature and exposed to the exciting laser pulses while a series of <sup>1</sup>Δ<sub>g</sub> emission traces were recorded to detect any production of oxygen in the sample over a period of 2 h.

## Results

**Transformation of C<sub>60</sub>X to C<sub>60</sub>O.** The top frame of Figure 1 shows three out of a total of eleven chromatograms obtained from experiment 8 (in toluene at 0.4 °C), taken at increasing reaction times. Absorption spectra indicate that the peak labeled C<sub>60</sub>X contains only one species. At sufficiently long times, all C<sub>60</sub>X transformed to C<sub>60</sub>O and no other compounds were observed. In the run shown here, C<sub>60</sub> was absent at the beginning and was not formed during the transformation; hence the peak areas and heights of both C<sub>60</sub>X and C<sub>60</sub>O were normalized to their sums, which remained constant within a few percent. Data points in the bottom frame of Figure 1 show HPLC peak heights for C<sub>60</sub>X and C<sub>60</sub>O as a function of time in this experiment. The solid curves are best-fit simulations using kinetic models for first-order decay and growth. The deduced rate constants of 2.44 × 10<sup>-3</sup> and 2.46 × 10<sup>-3</sup> min<sup>-1</sup>, respectively, match each other very closely. Similar first-order decay of C<sub>60</sub>X and growth of C<sub>60</sub>O were observed in all 12 experiments; we list the corresponding rate constants in Table 1 (*k* for C<sub>60</sub>X decay and *k'* for C<sub>60</sub>O growth). Figure 2 is an Arrhenius plot of the temperature-dependent rate constants in toluene. The linear fit through these data implies an activation energy of 89 ± 7 kJ

(3) Adjustments to the flow rate were made to maintain pressures below 2500 psi.

(4) The hexane solution was used only to prepare purified C<sub>60</sub>X by HPLC.

(5) Estimated from the C<sub>60</sub>O concentration after completion of the experiment.

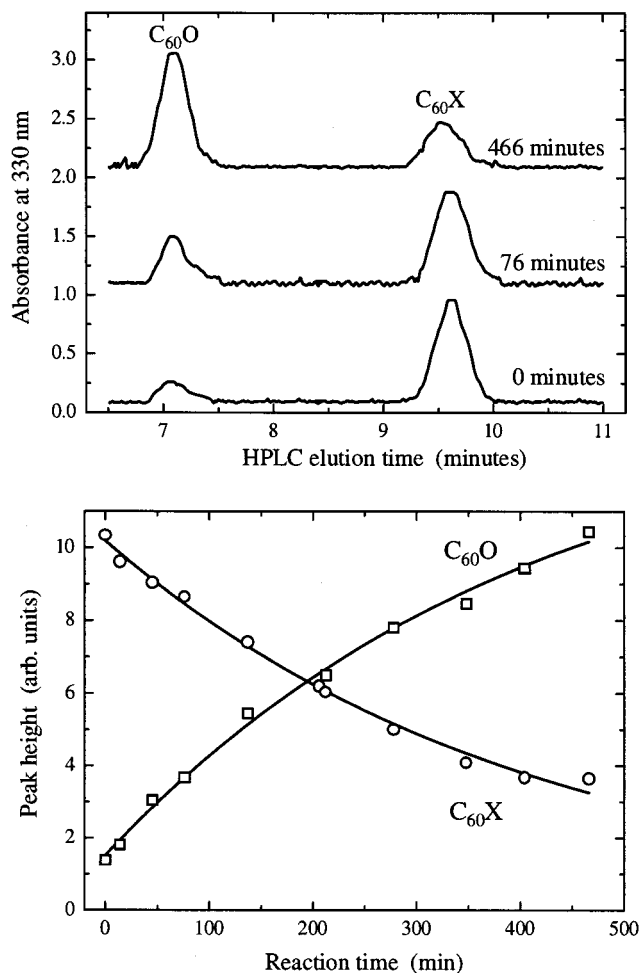


**Figure 1.** Top frame: Three 330 nm HPLC chromatograms from run no. 8 ( $0.4\text{ }^\circ\text{C}$  in toluene) taken at reaction times of 0, 76, and 466 min. The mobile phase was toluene at a flow rate of 1.5 mL/min. The peak at 7.2 min is due to  $C_{60}O$  and that at 9.6 min is due to  $C_{60}X$ . Traces have been displaced vertically by 1 au for clarity. Bottom frame: Heights of the  $C_{60}O$  and  $C_{60}X$  HPLC peaks as a function of reaction time, with solid curves showing best-fit first-order kinetic simulations.

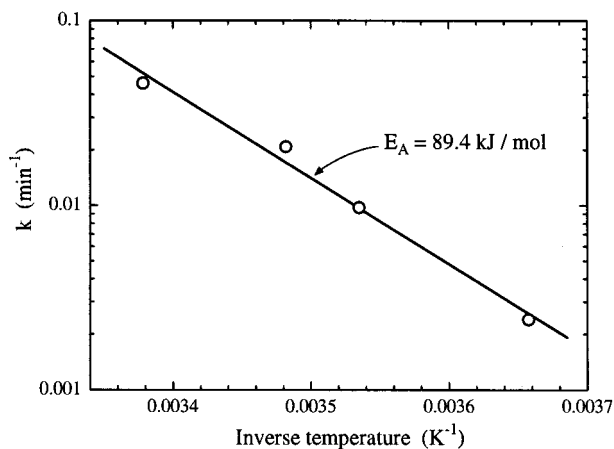


**Figure 2.** Arrhenius plot of the first-order rate constants found from HPLC data for the transformation of  $C_{60}X$  into  $C_{60}O$  in toluene solution. The solid line is a linear best fit.

$\text{mol}^{-1}$  ( $21 \pm 2\text{ kcal mol}^{-1}$ ) for the thermal transformation of  $C_{60}X$  to  $C_{60}O$ . The Arrhenius pre-factor falls in the range of  $3 \times 10^{11}$  to  $1 \times 10^{14}\text{ s}^{-1}$  (10 to 3500  $\text{cm}^{-1}$ ), as is consistent with unimolecular dissociation through vibrational motion.

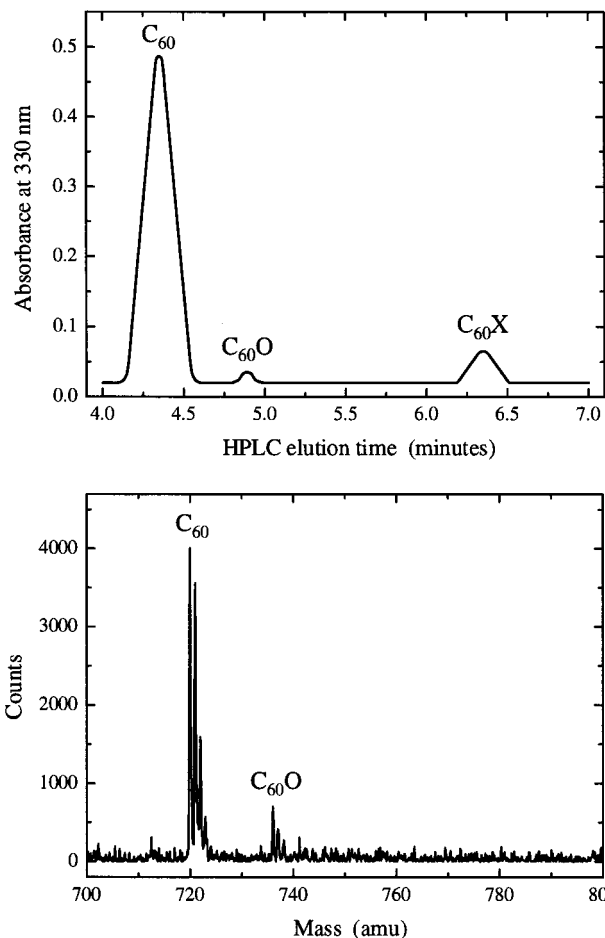


**Figure 3.** Top frame: HPLC chromatogram of a freshly ozonized sample of  $C_{60}$  in isooctane. Bottom frame: Laser-desorption time-of-flight mass spectrum of the same sample, taken in reflectron mode.

The main difference between the results of experiments 1 to 8 and 9 to 12 was that only  $C_{60}O$  was produced in the first series, whereas small amounts of  $C_{60}O_2$ [I] and  $C_{60}O_2$ [II] were also formed in the second series.<sup>6</sup> The concentration of  $C_{60}O_2$ -[II], like that of  $C_{60}O$ , was observed to increase with time. The growth of  $C_{60}O_2$ [I] could not be monitored because it had almost the same HPLC retention time as  $C_{60}X$ . It was demonstrated by the ozonation of pure  $C_{60}O$  in toluene that the formation of these dioxides was not due to a branched decay of  $C_{60}X$ , but rather to the presence in ozonized solutions 9 to 12 of several unstable compounds, collectively named  $C_{60}Y$ , whose retention times were longer than that of  $C_{60}X$  and which transformed to  $C_{60}O_2$ [I] and  $C_{60}O_2$ [II].<sup>7</sup> The only transformation of  $C_{60}X$  in all 12 experiments was first-order decay to  $C_{60}O$ .

As in the case of the samples in toluene and octane solution, solid  $C_{60}X$  transformed to  $C_{60}O$  by first-order kinetics. The rate constant at  $23\text{ }^\circ\text{C}$  was  $2.95 \times 10^{-3}\text{ min}^{-1}$ , which is a factor of 1.6 smaller than in toluene but 23 times larger than in octane at the same temperature.

**Mass Spectrometry.** Figure 3 shows the HPLC chromatogram and mass spectrum of a sample of  $C_{60}$  in isooctane, measured immediately after ozonation. It is seen that although  $C_{60}$ ,  $C_{60}O$ , and  $C_{60}X$  all appear in the chromatogram, the mass spectrum shows only peaks of  $C_{60}$  (at  $m/z$  720 to 724 amu) and of  $C_{60}O$  (at  $m/z$  736 to 738 amu). The sample solution was stored

(6) If  $C_{60}O_2$ [III] and  $C_{60}O_2$ [I] had been present in the analysis shown in Figure 1, their retention times would have been 8.1 and 9.7 min, respectively.

(7) Heymann, D.; Cataldo, F. *Fullerene Sci. Technol.* Manuscript submitted March 2000.

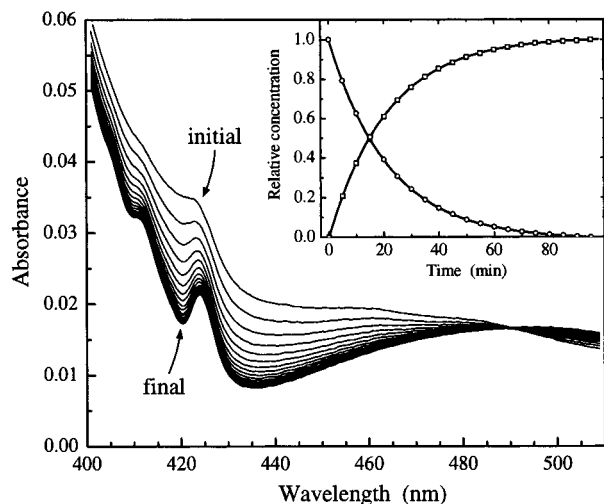


**Figure 4.** Absorption spectra of a solution of  $C_{60}X$  ( $C_{60}O_3$ ) in toluene taken at 5-min intervals as it transformed into  $C_{60}O$ . Inset: Points show the amplitudes as a function of time for two spectral components that describe the evolving spectra. The solid lines are first-order kinetic simulations of the appearance and decay of these components. Both fits give a decay constant of  $4.61 \times 10^{-2} \text{ min}^{-1}$ .

at 21 °C and sampled after 1.5, 3.5, and 72 h for HPLC and mass spectral analyses. Whereas the additional chromatograms showed the expected transformation of  $C_{60}X$  to  $C_{60}O$ , there was very little change in the mass spectra and no new mass peaks appeared. Qualitatively identical results were found for ozonized solutions of  $C_{60}$  in toluene and hexane.

**UV-vis Spectroscopy.** The near-ultraviolet spectrum of a toluene solution of  $C_{60}X$  showed significant changes during the transformation to  $C_{60}O$ , as the absorption maximum shifted from 325.8 to 328.5 nm. The main frame of Figure 4 displays a sequence of scans in the 400 to 500 nm region. Here one can see the evolution of a broad shoulder near 423.5 nm into the sharp 424 nm peak characteristic of  $C_{60}O$ . The clear isosbestic point at 490 nm and another at 312.3 nm strongly suggest that only a single fullerene species is produced by decay of  $C_{60}X$ . From the presence of a broad maximum near 500 nm for the product but not the reactant, we deduce that the derivatized carbon atoms of  $C_{60}X$  are not part of a three-membered ring, as in the epoxide  $C_{60}O$  or methanofullerenes. In addition, a band at 680 nm decreases in intensity during the transformation, ruling out a [5,6]-open fulleroid structure for  $C_{60}X$ . These spectra indicate that  $C_{60}X$  is a [6,6]-closed  $C_{60}$  derivative that lacks a three-membered ring, and that it transforms into the  $C_{60}O$  epoxide with no significant fullerene side-products.

We analyzed each UV-vis spectrum taken during the transformation as a linear combination of the final and initial spectra, and then performed a kinetic analysis on the deduced coefficients. The result, plotted in the inset of Figure 4, shows very accurate first-order kinetics with a rate constant of  $4.61 \times 10^{-2} \text{ min}^{-1}$  at 296 K. This value is in excellent agreement with the result from HPLC kinetics.

Because some decay of  $C_{60}X$  to  $C_{60}O$  had already occurred by the time the first spectral scan was begun on an isolated  $C_{60}X$  fraction, we could not obtain a spectrum of the pure intermediate by that method. Instead, we used the photodiode array detector of a Shimadzu HPLC to measure the  $C_{60}X$  spectrum as that fraction eluted from the column. Figure 5 shows the resulting spectra of  $C_{60}X$  and  $C_{60}O$ , scaled to give proper isosbestic wavelengths and therefore accurate relative absorptivities.

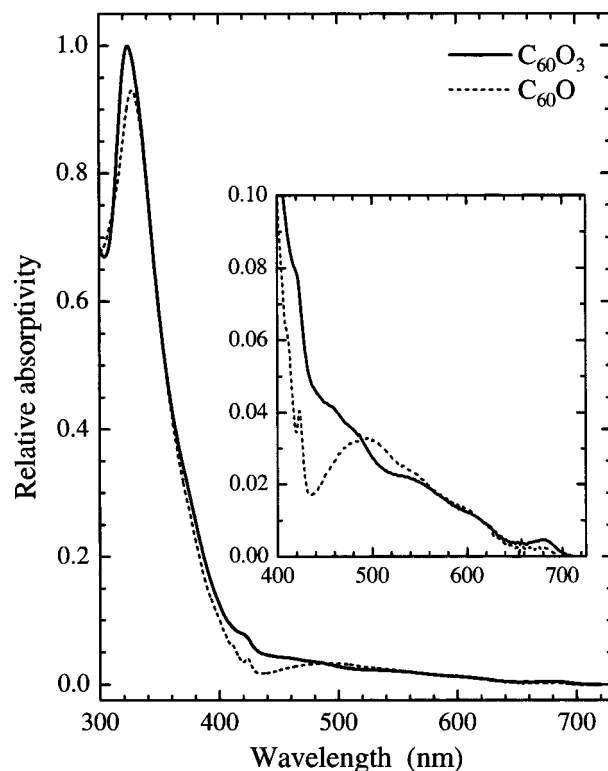


**Figure 5.** Absorption spectra of (solid curve)  $C_{60}X$  ( $C_{60}O_3$ ) and (broken curve)  $C_{60}O$  in room-temperature toluene solution. The two spectra have been scaled to show correct relative molar absorptivities. The inset shows an expanded view of the longer-wavelength region.

**Oxygen Release.** Generation of molecular oxygen from  $C_{60}X$  was investigated using the sensitized photoluminescence method described above. The  $C_{60}X$  HPLC fraction from a freshly ozonized  $C_{60}$  solution in toluene was collected, degassed, and sealed in an optical cell. We estimated the initial  $C_{60}X$  concentration in this 23 °C sample to be approximately 40  $\mu\text{M}$ . Irradiation at 532 nm induced detectable 1270 nm oxygen luminescence, the intensity of which increased over a period of 6 min. To estimate the final concentration of dissolved oxygen, we waited 115 min for the reaction to run to completion, recorded the oxygen luminescence trace labeled “after reaction” in Figure 6, and then opened the cell to the atmosphere. When equilibration with atmospheric  $O_2$  was complete, we observed the increased sensitized luminescence signal labeled “air-saturated” in Figure 6. To check that the source of the detected oxygen was in fact the transforming  $C_{60}X$ , we took the fully converted sample, degassed it thoroughly, waited for more than 65 min, and then measured the “blank” trace in Figure 6. This sensitized 1270 nm luminescence is clearly only a small fraction of what had been observed earlier from the same sample, confirming that the “after reaction” oxygen signal did not arise from cell leaks or outgassing, but rather from the  $C_{60}X$ .

Analysis of these traces showed an intensity enhancement of 3.6 on increasing the dissolved  $O_2$  concentration from the level produced by  $C_{60}X$  decay to the  $2.1 \times 10^{-3} \text{ M}$  level of air-saturated toluene.<sup>8</sup> After  $C_{60}X$  transforms to  $C_{60}O$ , the  $C_{60}O$  product should act as a short-lived trap for all fullerene triplet energy in the sample cell. Sensitization of oxygen therefore requires bimolecular quenching of triplet  $C_{60}O$  in competition with its unimolecular decay constant ( $k_1$ ) of  $2 \times 10^5 \text{ s}^{-1}$ .<sup>9</sup> The

(8) Murov, S. L.; Carmichael, I.; Hug, G. L. *Handbook of Photochemistry*; Marcel Dekker: New York, 1993.

(9) Benedetto, A. F.; Weisman, R. B. *Chem. Phys. Lett.* **1999**, *310*, 25–30.

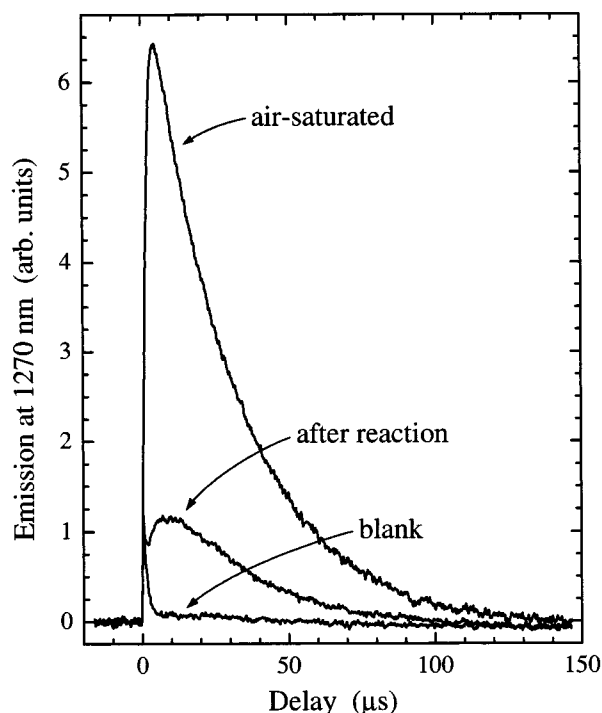


**Figure 6.** Time-resolved 1270 nm emission signals from a sample of C<sub>60</sub>X (C<sub>60</sub>O<sub>3</sub>) in toluene at 296 K following pulsed optical excitation. The “after reaction” curve was measured in a sample that had been degassed and then allowed to react for 115 min. The “air-saturated” curve was measured in the same sample after subsequent equilibration with atmospheric oxygen. The “blank” curve was measured after the reacted solution was degassed again and allowed to stand for more than 65 min. Other experimental conditions remained the same for these runs. (The small fast-decaying components visible in the “after reaction” and “blank” curves reflect weak fluorescence emission rather than singlet oxygen luminescence.)

fraction of triplet C<sub>60</sub>O molecules that sensitize oxygen is simply

$$\phi_{\text{sens}} = \frac{k_q[\text{O}_2]}{k_1 + k_q[\text{O}_2]} \quad (1)$$

where  $k_q$  is the rate constant for triplet quenching by oxygen (ca.  $1.6 \times 10^9 \text{ M}^{-1} \text{ s}^{-1}$  for fullerenes). The  $\phi_{\text{sens}}$  value when  $[\text{O}_2]$  was equal to  $2.1 \times 10^{-3} \text{ M}$  was found to be 3.6 times that when it equaled the final concentration in the sample cell. Using this ratio, eq 1, and the given rate constants, we find a final oxygen concentration of  $44(\pm 10) \mu\text{M}$ , a value that matches the initial concentration of C<sub>60</sub>X. We therefore deduce that each molecule of C<sub>60</sub>X released one molecule of O<sub>2</sub> as it transformed into C<sub>60</sub>O.

## Discussion

A key question is the identity of the intermediate species, C<sub>60</sub>X. Three plausible candidates are the [5,6]-open C<sub>60</sub>O fulleroid, yet another isomer of C<sub>60</sub>O<sub>2</sub>, or an ozonide C<sub>60</sub>O<sub>3</sub>. We can rule out the [5,6]-open fulleroid structure of C<sub>60</sub>O, because fulleroids do not show absorption bands near 680 nm,<sup>10</sup> and that species obviously could not liberate oxygen when transforming to the [6,6]-closed epoxide derivative. If C<sub>60</sub>X were a dioxide of C<sub>60</sub>, it might generate O<sub>2</sub> while converting to C<sub>60</sub>O,

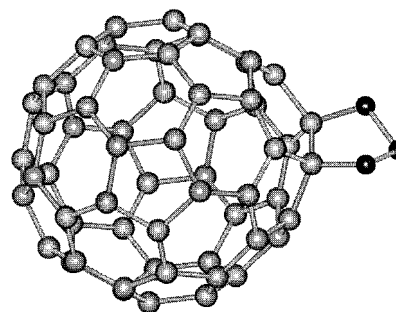


**Figure 7.** Equilibrium ground-state structure of the ozonide C<sub>60</sub>O<sub>3</sub> computed using the PM3 RHF method.

but that process would most likely follow second-order rather than the observed first-order kinetics and would generate only half as much O<sub>2</sub> as was detected. The remaining candidate, C<sub>60</sub>O<sub>3</sub> ozonide, is consistent with the measured amount of evolved O<sub>2</sub> and also with the UV–visible spectrum of C<sub>60</sub>X, whose features suggest a [6,6]-closed C<sub>60</sub> derivative lacking a three-membered ring. Identification of C<sub>60</sub>X as C<sub>60</sub>O<sub>3</sub> also explains why the HPLC retention times of C<sub>60</sub>X and C<sub>60</sub>O<sub>2</sub>[I] are almost equal and exceed that of C<sub>60</sub>O. On the Cosmosil Buckyprep column, longer retention times of fullerenes and derivatized fullerenes usually imply higher mass, larger dipole moments, or both. C<sub>60</sub>O<sub>3</sub> and C<sub>60</sub>O<sub>2</sub>[I] clearly have greater masses and perhaps also larger dipole moments than C<sub>60</sub>O. The conclusion that C<sub>60</sub>X is C<sub>60</sub>O<sub>3</sub> seems inconsistent only with the mass spectrum of Figure 3, which shows no species of mass higher than  $m/z$  736 amu (C<sub>60</sub>O). However, we think that this negative result merely reflects the difficulty of obtaining laser desorption mass spectra of rather labile compounds. In our kinetic studies, we have observed that optical irradiation significantly accelerates C<sub>60</sub>X decay. Exposure of the mass spectrometry samples to the desorption laser beam may therefore have caused both thermal and photodissociation of C<sub>60</sub>O<sub>3</sub>, preventing C<sub>60</sub>O<sub>3</sub><sup>+</sup> ions from reaching the detector. We conclude that our experimental results identify C<sub>60</sub>X as the ozonide, C<sub>60</sub>O<sub>3</sub>.

We have computationally explored the structure and stability of C<sub>60</sub>O<sub>3</sub> using semiempirical PM3 RHF calculations in HyperChem v.5.11 (HyperCube, Inc.). Interestingly, some of the fully optimized PM3 structures and energies differ significantly from those of a recent AM1 study by Shang et al.<sup>1p</sup> Our structure for the primary ozonide C<sub>60</sub>O<sub>3</sub>, shown in Figure 7, has C<sub>s</sub> symmetry and C–O bond lengths of 141.8 pm. The 159.6 pm separation and 0.9 bond order between the derivatized carbon atoms suggests a weak residual single bond at the [6,6] ring fusion. We find that the O<sub>3</sub> moiety in C<sub>60</sub>O<sub>3</sub> has O–O bond lengths of 148.3 pm, a value typical of actual O–O single bonds,<sup>11</sup> but much larger than the AM1 value of 130.7 pm. Note that the 127.2 pm experimental O–O bond length in free ozone<sup>12</sup> is much closer to the PM3 value of 122.3 pm than to the AM1 value of 116.0 pm. Similarly, the O<sub>2</sub> bond length is underestimated by 12.2 pm in AM1 but only by 3.9 pm in PM3. Our PM3-calculated O–O–O angle in C<sub>60</sub>O<sub>3</sub> is 100.7°, as compared to 108.0° in the AM1 work of Shang et al.<sup>1p</sup> and 116.8° in free ozone. The primary ozonide therefore shows substantially more bonding between O<sub>3</sub> and C<sub>60</sub> moieties in our calculations than was predicted by the AM1 method.

(10) (a) Smith, A. B., III; Strongin, R. M.; Brard, L.; Furst, G. T.; Romanow, W. J. *J. Am. Chem. Soc.* **1993**, *115*, 5829–5830. (b) Janssen, R.; Hummelen, J. C.; Wudl, F. *J. Am. Chem. Soc.* **1995**, *117*, 544–545. (c) Ceroni, P.; Conti, F.; Corvaja, C.; Maggini, M.; Paolucci, F.; Roffia, S.; Scorrano, G.; Toffoletti, A. *J. Phys. Chem.* **2000**, *104*, 156–163.

(11) Greenwood, N. N.; Earnshaw, A. *Chemistry of the Elements*; Pergamon: Oxford, 1984; p 720.

(12) Harmony, M. D.; Laurie, V. W.; Kuczkowski, R. L.; Schwendeman, R. H.; Ramsay, D. A. *J. Phys. Chem. Ref. Data* **1979**, *8*, 619–721.

**Table 2.** Computed Ground State Energies of Various C<sub>60</sub>O<sub>3</sub> Species Relative to the Energy of Separated C<sub>60</sub> and O<sub>3</sub><sup>a</sup>

compd	energy (kJ mol <sup>-1</sup> )
C <sub>60</sub> + O <sub>3</sub>	0
[6,6]-closed C <sub>60</sub> O <sub>3</sub>	-280
[5,6]-closed C <sub>60</sub> O <sub>3</sub>	-201
[6,6]-closed C <sub>60</sub> O + O <sub>2</sub> ( <sup>3</sup> Σ <sub>g</sub> <sup>-</sup> )	-315
[6,6]-closed C <sub>60</sub> O + O <sub>2</sub> ( <sup>1</sup> Δ <sub>g</sub> )	-221

<sup>a</sup> All values were obtained from geometry-optimized PM3 RHF calculations.

This bonding difference is also evident from the relative energies listed in Table 2, as our work shows the formation of [6,6]-C<sub>60</sub>O<sub>3</sub> from C<sub>60</sub> and ozone to be exothermic by 280 kJ mol<sup>-1</sup>, or almost twice the 141 kJ mol<sup>-1</sup> value reported using AM1.<sup>1p</sup> A [5,6]-closed primary ozonide is calculated to be less stable than the [6,6]-adduct. We calculate that dissociation of the [6,6]-C<sub>60</sub>O<sub>3</sub> primary ozonide into C<sub>60</sub>O and ground state (<sup>3</sup>Σ<sub>g</sub><sup>-</sup>) O<sub>2</sub> is exothermic by 35 kJ mol<sup>-1</sup>. However, this process is spin-forbidden. There are also two possible dissociation channels that are spin-allowed but activated. One produces O<sub>2</sub> in its <sup>1</sup>Δ<sub>g</sub> excited state, which lies 94 kJ mol<sup>-1</sup> above <sup>3</sup>Σ<sub>g</sub><sup>-</sup>. The similarity between this O<sub>2</sub> excitation energy and the experimental activation energy of 89 kJ mol<sup>-1</sup> suggests that it may be the dominant pathway for C<sub>60</sub>O<sub>3</sub> dissociation. The second spin-allowed channel requires electronic excitation of C<sub>60</sub>O<sub>3</sub> to its lowest triplet state, after which exothermic dissociation into ground-state C<sub>60</sub>O and (<sup>3</sup>Σ<sub>g</sub><sup>-</sup>) O<sub>2</sub> may be very rapid. This channel might be expected to give C<sub>60</sub>O<sub>3</sub> a high quantum yield of photodissociation, as seems indicated by preliminary observations in our laboratory.

The C<sub>60</sub>O<sub>3</sub> structure shown in Figure 7 is a 1,2,3-trioxolane, or primary ozonide. It is believed that primary ozonides are formed by concerted 1,3-dipolar cycloaddition of ozone to a double bond. Once formed, many organic primary ozonides undergo complete cleavage of the C–C bonds, apparently through a carbonyl oxide intermediate, to give 1,2,4-trioxolane structures termed ozonides.<sup>13</sup> In the case of C<sub>60</sub>O<sub>3</sub>, however, production of such a 1,2,4-trioxolane would require that one or two oxygen atoms penetrate into the fullerene cage. The C<sub>60</sub>O<sub>3</sub> primary ozonide is instead observed to undergo efficient partial cleavage to form an epoxide and molecular oxygen.

The HPLC kinetic results on the transformation of C<sub>60</sub>O<sub>3</sub> to C<sub>60</sub>O + O<sub>2</sub> (Table 1) show that the reaction is much faster in toluene than in octane at the same temperature, a clear case of strong solvent effects. Such effects on reaction rates of fullerene derivatives are known for other systems, and have been tentatively explained by the formation of weak ground-state complexes of the derivatized fullerenes and aromatic solvent molecules through π–π interactions.<sup>14</sup> It appears that such interactions make C<sub>60</sub>O<sub>3</sub> more prone to decay in toluene than in octane. Although the transformation is slightly slower in the solid state than in toluene, it is still an order of magnitude faster than in octane. It seems that the transformation in the solid state may be accelerated relative to that in octane by π–π interactions between neighboring fullerene molecules.

The finding that C<sub>60</sub>X is an ozonide strengthens the hypothesis that the unstable products labeled C<sub>60</sub>Y are also ozonides such as C<sub>60</sub>O(O<sub>3</sub>) or C<sub>60</sub>(O<sub>3</sub>)<sub>2</sub>,<sup>7</sup> and sheds fresh light on the nature

(13) Bailey, P. S. *Ozonation in Organic Chemistry*; Academic Press: New York, 2000; Vol. I.

(14) (a) Seshadri, R.; Rao, C. N. R.; Pal, H.; Mukherjee, T.; Mittal, J. P. *Chem. Phys. Lett.* **1993**, *205*, 395–398. (b) Rath, M. C.; Pal, H.; Mukherjee, T. *J. Phys. Chem. A* **1999**, *103*, 4993–5002.

and formation of the insoluble substances that commonly form on ozonation of C<sub>60</sub> in nonpolar solvents.<sup>1b–h,j–m</sup> Several of the chemical and physical properties of these substances have been reported elsewhere.<sup>15</sup> New laser-desorption mass spectrometric measurements made in the present study strongly suggest that these solids contain heavily substituted carbon-bearing units with masses up to about 4000 amu,<sup>16</sup> and additional electron-ionization mass spectra show that mainly H<sub>2</sub>O<sup>+</sup>, CO<sub>2</sub><sup>+</sup>, COOH<sup>+</sup>, and C<sub>3</sub>OOH<sup>+</sup> ions are observed when the solids are heated from 60 to 600 °C. Electron microscopy showed that the solids have atomic O/C ratios of 0.5.<sup>15</sup> Although a C<sub>60</sub> molecule has thirty [6,6] C–C bonds, the insoluble compounds cannot be (C<sub>60</sub>O<sub>30</sub>)<sub>n</sub> “super-[6,6]-epoxide” oligomers, because FTIR and NMR spectra show clearly that fullerene cage rupture has occurred.<sup>15</sup> The identified functional groups include C=O, C–OH, C–O–C, and COOH.<sup>15,17</sup>

A fundamental issue is therefore the mechanism of cage rupture during ozonation. The present work shows that the first O<sub>3</sub> molecule attached to a [6,6] C–C bond readily loses O<sub>2</sub> to form the mono-epoxide, leaving intact the [6,6] C–C bond. C<sub>60</sub>O<sub>3</sub> reaction paths leading to carbonylation are not observed. However, if an O<sub>3</sub> molecule attacks one of the sixty [5,6] C–C bonds (perhaps after derivatization of several [6,6]-sites) the underlying C–C bond is likely to break and may not re-form on release of O<sub>2</sub>. Among the consequences of this process could be the formation of C=O groups and reaction with H<sub>2</sub>O in the solvent to form C–OH and COOH groups. After treatment with large amounts of ozone, solutions of C<sub>60</sub> in nonpolar solvents were found to contain no C<sub>60</sub>, C<sub>60</sub>O<sub>3</sub>, or higher ozonides; and no C<sub>60</sub>O or higher oxides were observed to form by the decay of intermediates. Instead, the C<sub>60</sub> reactant is quantitatively transformed to insoluble matter with a total mass increase of approximately a factor of 2. These observations are consistent with the reaction scheme proposed above and suggest that the chemically reactive zones of derivatized C<sub>60</sub> may also contribute to C–O–C linkage between cages. These species should not be viewed as derivatized but otherwise intact fullerenes, but rather as C<sub>60</sub> molecules in various stages of disintegration. Consequently, the transformation of C<sub>60</sub> to insoluble matter is probably much more complex than sequential oxidation of C<sub>60</sub> to form C<sub>60</sub>O<sub>n</sub> (n = 1, 2, ..., 6) ending with cage rupture at C<sub>60</sub>O<sub>7</sub>, a mechanism that had been proposed several years ago by Heymann and Chibante.<sup>1b,18</sup>

## Conclusions

We have found that the [6,6]-closed epoxide C<sub>60</sub>O is not formed directly through ozonation of C<sub>60</sub> in solution, but rather through the decay of an intermediate adduct that has been identified as C<sub>60</sub>O<sub>3</sub>, a [6,6]-closed primary ozonide. This intermediate, which is the first fullerene ozonide to be reported, dissociates by first-order kinetics with a room-temperature lifetime on the order of 100 min and an activation energy in toluene of ~89 kJ mol<sup>-1</sup>. We have measured the evolution of one molecule of O<sub>2</sub> per molecule of C<sub>60</sub>O<sub>3</sub> as it dissociates to form C<sub>60</sub>O. The UV–vis spectrum of C<sub>60</sub>O<sub>3</sub> shows features

(15) Heymann, D.; Cataldo, F. *Polymer Degradation and Stability*, in press.

(16) However, the most abundant ions in the spectrum cannot contain the carbon atoms from more than one or two C<sub>60</sub> molecules.

(17) 5.0 mg of product dissolved in 50 mL of water showed a pH of 3.76.

(18) Unstable compounds were never observed by these investigators because they always allowed the ozonized solutions to “settle” for several hours, by which time all C<sub>60</sub>X and C<sub>60</sub>Y ozonides had already transformed to stable oxides.

consistent with a [6,6]-closed adduct, in agreement with the equilibrium structure predicted by semiempirical quantum chemical calculations. Identification of the ozonide intermediate suggests a mechanism for the formation of heavily oxygenated polymeric products in the reaction of C<sub>60</sub> with large amounts of ozone.

It seems likely that ozonides of C<sub>60</sub> derivatives and of higher fullerenes can be prepared and studied using methods similar to the ones employed here. There is also reason to expect that this family of compounds may show intriguing properties, including solvent-dependent stabilities and high quantum yields

of photodissociation to liberate O<sub>2</sub>. Investigations of C<sub>70</sub> ozonation products are currently underway.

**Acknowledgment.** We thank W. E. Billups and R. J. Parry of the Department of Chemistry of Rice University for access to their HPLC and ozonation apparatus and J. Dijkink of the Department of Chemistry of the University of Amsterdam for the use of his ozonation equipment. R.B.W. and S.M.B. are grateful to the National Science Foundation and the Welch Foundation for support of this research.

JA0025651